JOURNAL OF CATALYSIS 148, 47–55 (1994)

CO and NO Interaction with Pd–Ag and Pd–Cr Bimetallic Catalysts

I. X-Ray Diffraction, Infrared Spectroscopy, and Thermoreaction

A. El Hamdaoui, G. Bergeret, J. Massardier, M. Primet, and A. Renouprez[1]

Institut de Recherches sur la Catalyse (CNRS), 2 Avenue A. Einstein, 69626 Villeurbanne Cedex, France

Received April 6, 1993; revised December 6, 1993

Well-defined Pd-based bimetallic catalysts have been prepared and characterized. X-ray diffraction shows that in Pd–Ag, Ag has a strong tendency to segregate at the surface of the catalyst. On the other hand, in Pd–Cr, Cr is well distributed in the network of Pd and induces an electronic structure modification of Pd. The adsorption and coadsorption of CO and NO on these solids were studied by infrared spectroscopy and thermodesorption and compared with similar adsorptions on pure palladium and rhodium. It was shown that although the adsorption energies of CO and NO on the various catalysts are similar, upon coadsorption of the two reactants the surface coverage by NO is 4 to 20 times larger than by CO. Silver decreases this CO coverage and chromium slightly increases it. When a thermoreaction is performed at 430 K, appreciable amounts of N_2 and CO_2 are evolved from Pd, Pd–Cr, and Rh catalysts; Pd–Cr is more reactive than Pd and Pd–Ag is unreactive.

INTRODUCTION

It is well known that in the catalytic conversion of NO by CO, rhodium is the most active of all precious metals (1). For the oxidation of CO, platinum is generally considered as the most efficient. These two metals are thus associated in most exhaust catalysts (2, 3). Palladium, although less efficient than rhodium in the former reaction, could be a good basis for a new type of bimetallic system if its selectivity for NO reduction could be increased by the presence of a second metal. Following this approach, silver was chosen as a second metal because of its properties of modification of CO adsorption and its ability to promote selective oxidation (4). On the other hand, as shown recently (5), chromium strongly modifies the electronic structure of palladium and thus one can expect that the chemisorption of NO would be promoted. Pd–Cr was therefore also chosen for study.

In this first paper the chemisorptive properties of these solids for CO and NO are reported. The coadsorption of the two reactants on the bimetallic catalysts at several temperatures is compared with the adsorption on palladium and rhodium. The chemisorbed species have been studied by infrared spectroscopy and the reaction occurring between them on temperature increase was followed by mass spectroscopy.

[1] To whom correspondence should be addressed.

EXPERIMENTAL

(I) Catalyst Preparation

Palladium–silver catalysts. The silica support was coimpregnated with the corresponding nitrates and the choice of the optimum conditions of reduction were selected after *in situ* X-ray experiments had been performed under hydrogen at several temperatures.

Palladium and palladium–chromium catalysts. The preparation and characterization of these samples have been described in detail in previous work (5, 6). The support is a Degussa Aerosil 200 silica. The monometallic Pd catalyst was prepared by exchange with $Pd(NH_3)_4(OH)_2$ and after reduction at 600 K, the solid was impregnated with chromium nitrate. The solid was then reduced at 870 K. As shown by EXAFS, chromium is only reduced to 50% when supported on silica. The reduced metal forms a solid solution with palladium and the oxide coats the metallic particles.

Rhodium catalyst. The reference rhodium catalyst was prepared by impregnation of a Degussa (Oxyd C) nonporous γ-alumina with rhodium nitrate, followed by a reduction at 500 K under hydrogen.

(II) X-ray Diffraction

The formation of the Pd–Ag alloys upon heating under hydrogen was followed by *in situ* X-ray diffraction. The experiments were performed on a D500 Siemens goniometer equipped with a high temperature camera using Cu$K\alpha$ Ni-filtered radiation. This homemade stainless steel camera, closed by a water-cooled cylindrical Be window, is flushed with H_2 or He. The program-controlled temperature can reach 1000 K. The detector was a position-sensi-

0021-9517/94 $6.00

tive proportional counter (Raytech) covering a 16° (2θ) angular range. Compared to a conventional pinpoint detector, the sensitivity is improved by two orders of magnitude, which is especially valuable for weakly scattering materials such as 2% Pd supported catalysts with 1 to 5 nm metal particle size. The resolution of the instrument, measured with a silicon powder, is of the order of 0.15° (2θ) when the detector is in fixed position. The diffractograms were recorded in the step scan mode (step size 0.032°) within 2 h after a 2-h dwell at the required temperature. The background due to the silica support, which constitutes 80% of the total scattering, recorded over a 30° angular range was subtracted from the diffractogram using the Diffrac-AT software (Socabim). As it is necessary to scan this large angular range, the resolution is degraded to 0.25° due to parallax effects. The 35–50° (2θ) region was then adjusted with two Pearson functions to separate the contributions of the (111) and (200) lines of the solid solution after the subtraction of the contribution from the pure silver phase.

(III) Dispersion and Chemisorption

To determine the dispersion of the various catalysts, the particle diameter of the metallic phase was determined by electron microscopy and small angle X-ray scattering.

An indication of the composition of the surface and/or of its reactivity can be measured by its hydrogen chemisorption capacity, taking into account the areas determined by the physical methods. This was achieved by thermodesorption experiments using mass spectroscopy in the UHV instrument used for the CO–NO thermoreaction experiments. A calibration with an EuroPt sample is first performed. After activation at 600 K, the samples are outgassed at 700 K, hydrogen is chemisorbed at 300 K, and an evacuation at 300 K is performed before the thermodesorption experiment.

(IV) Infrared Spectroscopy

The IR measurements were performed with a Brucker IFS 110 FTIR instrument with a resolution of 4 cm^{-1} in the 1000–4000 cm^{-1} range. The samples, compressed under 2 × 10^5 kPa to obtain self-supported wafers (diameter 18 mm, weight 20–40 mg), can be treated under controlled atmosphere in the IR silica cell (closed by CaF_2 windows) before the introduction of CO or NO at 300 K at atmospheric pressure. Every spectrum results from the accumulation of 100 scans and the background of the support was subtracted using software facilities. The gas phase is eliminated by evacuation at 300 K, leaving a monolayer at the surface. The experiments lead to the relative amounts of adsorbed species and to the specific properties of the metals induced by alloying from the modifications of ν CO (7, 8) and ν NO (9) stretching frequencies.

7 MASSES (12, 14, 15, 16, 28, 30, 44)

NO		30		16	15	14	
N_2			28			14	
N_2O	44	30	28			14	
CO			28				12
CO_2	44		28	16			12

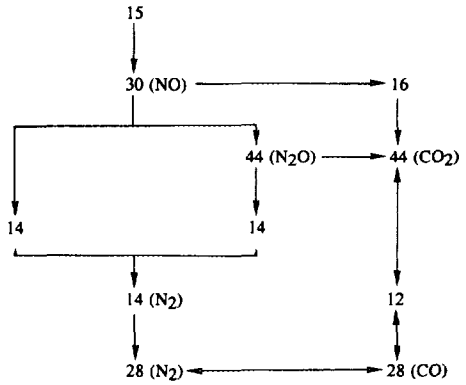

FIG. 1. Scheme of step-by-step analysis of the mass spectra.

(V) Thermoreaction and Thermodesorption

The experiments have been performed with a VG Micromass PC spectrometer connected to a UHV vessel evacuated by an Edwards oil diffusion pump and a VG CCT liquid nitrogen trap. After adsorption of the reactants at the desired temperature and evacuation at 10^{-6} Pa, the thermodesorption is carried out with a temperature rise of 40 K min^{-1}. To determine the relative amount of each reactant and product, namely CO, NO, N_2, CO_2, and N_2O, one needs to record 7 m/z values, i.e., 12, 14, 15, 16, 28, 30, and 44. In addition, the complete spectra of these 5 compounds and their respective sensitivity are required as standards. It was verified that the m/z = 14 peak corresponding to CO^{++} is not observed in the CO mass spectrum. Conversely, m/z = 15 corresponds to NO^{++}. The presence of such doubly ionized compounds actually depends on the adjustment of the mass spectrometer. Thus, from the m/z = 15 attributed unambiguously to NO, one is able, as shown in Fig. 1, to calculate step by step the contribution of each of the five reactants/products to the total spectrum.

RESULTS

(I) Formation of the Pd-Ag Alloys

Figure 2 shows the diffractograms obtained upon heating under H_2 at 490, 620, and 770 K. A solid solution is already formed at 490 K as demonstrated by the presence

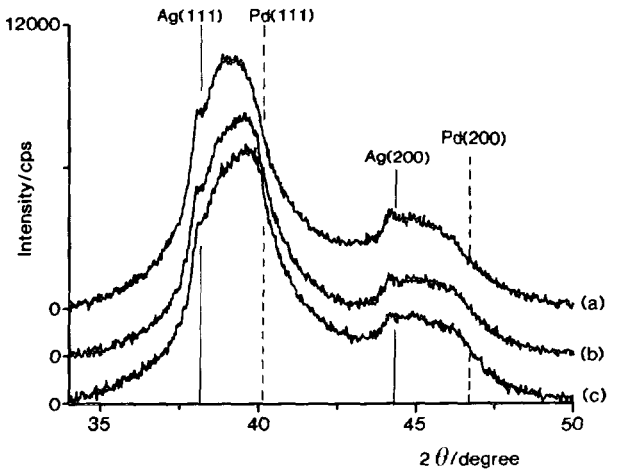

FIG. 2. X-ray diffraction patterns of Pd–Ag sample recorded under H_2: (a) at 490 K, (b) at 620 K, (c) at 770 K.

of (111) and (200) peaks located between the Bragg lines of pure Ag and Pd (Fig. 2a). The shoulder at the left of the (111) peak indicates that part of the silver is unalloyed. Actually after the decomposition using the Pearson functions (Fig. 3), this contribution was found to correspond to only 1.6% Ag, in the form of particles larger than 25 nm. After the subtraction of this contribution, the measured unit cell parameter of the solid solution corresponds to an Ag concentration of 46.5 ± 0.2% (10). The overall Ag concentration of 48.1% determined by diffraction is in excellent agreement with the 50% determined by chemical analysis and confirms the validity of the fitting procedure. The large width of the peaks is due to the small size of the particles and/or to a distribution of composition. Assuming tentatively that all the bimetallic particles have the same Pd–Ag composition, the width of the (111) peak gives an estimate of 3 nm for the size of the bimetallic particles. This value is smaller than that determined by SAXS and EM, which is actually the proof of a distribution of composition. When the temperature of reduction is raised to 620 K (Fig. 2b), the same decomposition leads to a silver concentration of 37.2% in the alloy and 1.2% of unalloyed Ag. This simultaneous decrease of pure silver and of silver concentration in the alloy can only be explained by the migration of part of Ag atoms from the bulk of the solid solution to the surface of the particles (11). This Ag surface migration is increased at 770 K (Fig. 2c), impoverishing the bulk concentration and thus shifting the diffraction line toward that of palladium and leading to a mean composition of Pd 65 ± 0.2, Ag 35 ± 0.2.

Figure 4 shows the diffractograms recorded after cooling the sample to 300 K under H_2. It is known (12) that the formation of the β-hydride which occurs on pure palladium has a stoichiometry which decreases when the silver concentration increases, and reaches zero for a silver concentration of 60%. Indeed, by comparing the diffractograms recorded under hydrogen at 490 K (Fig. 2a), a temperature where the hydride is destroyed, and at 300 K (Fig. 4a), the (111) peak is shifted to lower θ values by 0.5°, corresponding to an increase of the unit cell parameter of 0.05 Å due to hydrogen incorporation. From Ref. (12) it can be estimated that the solid solution $Pd_{53.5}$ $Ag_{46.5}$ can incorporate 0.15 hydrogen atom per metallic atom. For the higher temperatures of treatment, a shift between the diffractograms recorded at high temperature and at 300 K is also observed, proving that the hydride formation also takes place. However, this shift increases with the temperature of treatment, 0.65° for 620 K (Figs. 2b and 4b) and 0.75° for 770 K (Figs. 2c and 4c), corresponding to a parameter increase of 0.065 and 0.075 Å, respectively.

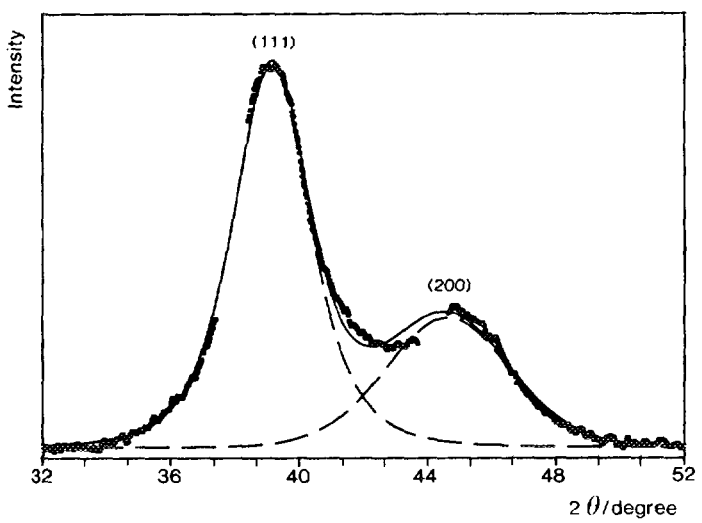

FIG. 3. Decomposition into two peaks (dashed and continuous lines) of the X-ray diffraction pattern of Fig. 2a (points), after subtraction of the diffraction of pure silver.

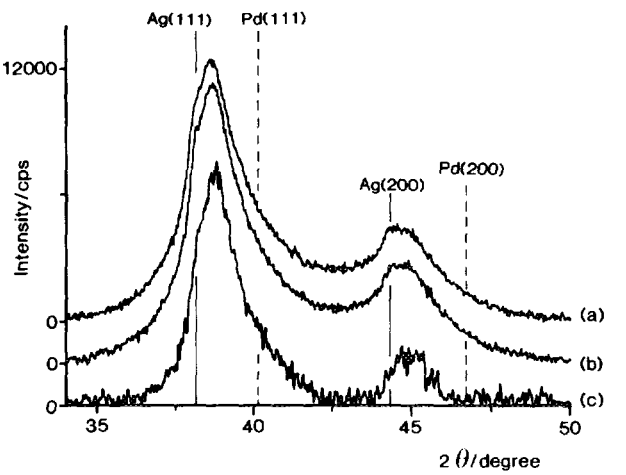

FIG. 4. X-ray diffraction patterns of Pd–Ag sample recorded at 300 K after cooling the samples under hydrogen from (a) 490 K, (b) 620 K, and (c) 770 K.

The hydrogen stoichiometries corresponding to the two compositions Pd_{63} Ag_{37} (620 K) and Pd_{65} Ag_{35} (770 K), interpolated from the data of Ref. (12), are 0.25 and 0.28. The widths of the peaks recorded at 300 K (Fig. 4) are smaller than those recorded at high temperature. This is due to the fact that the sample presents a distribution of composition. The silver-poor particles incorporate more hydrogen atoms than the silver-rich particles, and therefore give a larger angular shift. The particles with a silver concentration greater than 60% are not shifted as the hydride does not form. It incidentally occurs that the sum of these different shifted contributions leads to a sharpening of the peaks.

In conclusion, the XRD results have clearly shown a decrease of silver bulk concentration by migration of this element to the surface upon thermal treatment. The final treatment temperature of 770 K was chosen for the reaction experiments to ensure stability of the catalyst during the desorption experiments.

(II) *Chemisorption*

From inspection of Table 1, where the characteristics of the catalysts are summarized, it appears that the stoichiometry of 1 H atom per surface atom on the monometallic palladium catalyst is verified, whereas it is only 0.2 and 0.5 H atom per *surface metal atom* for the two bimetallic catalysts Pd–Ag and Pd–Cr. Two distinct explanations can be put forward.

For Pd–Ag, the nominal silver concentration is high enough to allow, by segregation at the surface of particles of only 25% dispersion, the formation of a silver-rich alloy (11), which was indeed confirmed by the X-ray study reported above. Moreover, silver being inactive in the dissociative chemisorption of hydrogen, the reduced chemisorption capacity of the Pd–Ag sample can be ascribed to the presence at the surface of an Ag-rich alloy.

Concerning Pd–Cr, the explanation is different. Taking into account the low Cr concentration, 13 at.%, and a dispersion of the metal measured by physical methods of 50%, even with the assumption of a complete surface segregation of chromium, its surface concentration cannot be higher than 25%. On the other hand, XPS does not detect any surface segregation of chromium. Thus, the decrease of the chemisorption cannot be attributed to a dilution of the palladium by unreactive chromium but rather, as shown in a previous work (5), to an electronic structure modification of the palladium.

TABLE 1

Characteristics of the Catalysts

Sample	Metal loading[a] (wt.%)	Diameter[b] (nm) EM	Diameter[b] (nm) SAXS	Hydrogen stoichiometry[c]
Pd/SiO_2	2.0	1.5	1.5	1.0
$Pd_{50}Ag_{50}/SiO_2$	2.25	5	5.0	0.2
$Pd_{87}Cr_{13}/SiO_2$	0.4	3	3.2	0.5
Rh/Al_2O_3	1.7	5		1.5

[a] Measured by chemical analysis.
[b] Surface averaged diameters.
[c] H atom/surface metallic atom.

(III) *Adsorption of CO at 300 K and Large Exposure*

As shown in Fig. 5a, the IR spectrum of CO adsorbed at 300 K on Pd/SiO_2 exhibits two main vibration modes, located at 2070 and 1975 cm^{-1}, generally attributed to linear and bridge-bonded CO (7, 8). Upon evacuation at 370 K, the former species, less strongly adsorbed, is preferentially evolved. An equal amount of CO is adsorbed under these two forms, as shown in the thermodesorption (TD) profiles of Fig. 6a, with desorption temperatures of 400 and 590 K. The presence of silver in palladium strongly decreases the amount of bridge or multibonded CO with a slight shift of frequency to lower wavenumber (Fig. 5b). This is confirmed by the thermodesorption spectrum of Fig. 6b, which shows a threefold decrease of the proportion of the species desorbing at high temperature and a shift of the desorption peaks to higher temperatures.

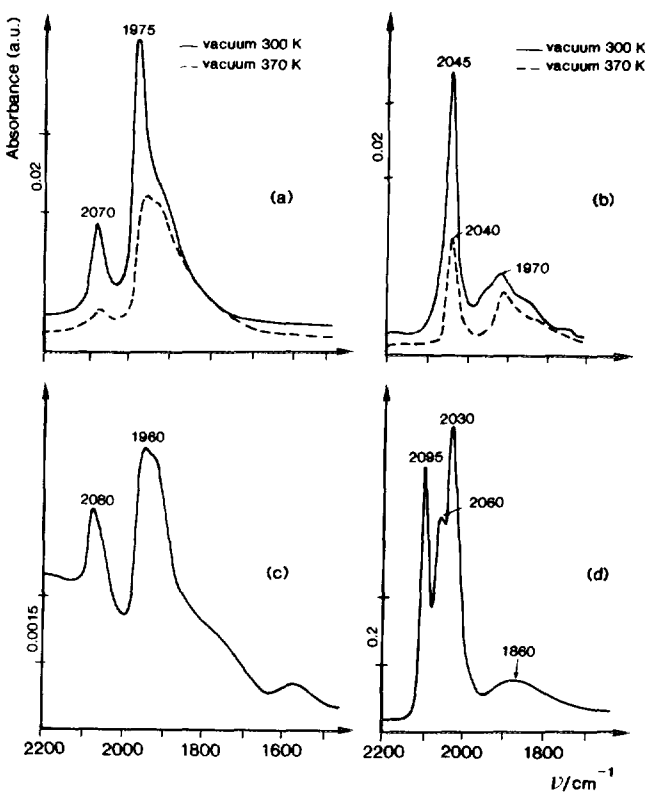

FIG. 5. IR spectra of CO adsorbed at 300 K: (a) on Pd, (b) on Pd–Ag, (c) on Pd–Cr, and (d) on Rh.

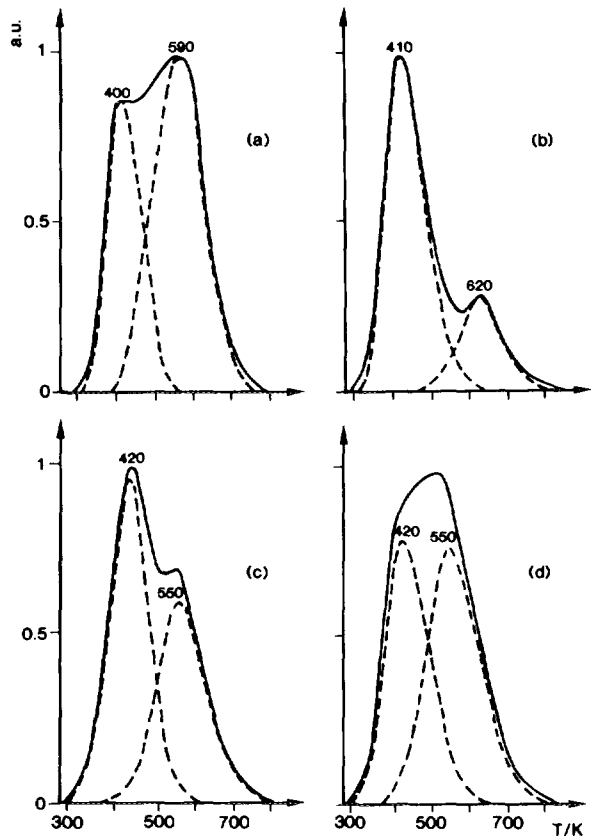

FIG. 6. Thermodesorption spectra of CO adsorbed at 300 K: (a) on Pd, (b) on Pd–Ag, (c) on Pd–Cr, and (d) on Rh.

On Pd–Cr, the situation is intermediate (Figs. 5c and 6c), with a slight reduction of the band attributed to the multibonded form (Fig. 5c).

On Rh/Al_2O_3, the IR spectrum shown in Fig. 5d is more complex and contains four distinct vibrations; besides the linear and the bridged forms observed at 2060 and 1860 cm^{-1} (9), the modes located at 2095 and 2030 cm^{-1} are generally attributed to a gem-dicarbonyl species (13). The TD spectrum represented in Fig. 6d is close to that of Fig. 6a, except that the two desorption peaks are now closer and separated by only 130 K. These results are summarized in Table 2.

(IV) Adsorption of NO at 300 K and at Large Exposure

By analogy with the chemistry of transition metal nitrosyls (14, 15), three types of bonding of the NO molecule with the metal surface need to be considered:

(i) Adsorption in the linear form, NO being bonded as an NO^+ species which is isoelectronic with CO. This type of adsorption leads to the formation of a ν NO band at wavenumbers above 1700 cm^{-1}.

(ii) Adsorption in the bridged structure, NO being bonded through the nitrogen end to two metal surface

TABLE 2

Thermodesorption of CO Adsorbed at 300 K

Sample	State I[a] T (K)	State II[a] T (K)	CO(II)/CO(I)
Pd/SiO_2	400	590	≈1.0
$Pd-Ag/SiO_2$	410	620	≈0.3
$Pd-Cr/SiO_2$	420	550	≈0.85
Rh/Al_2O_3	420	550	≈1.1

[a] State (I) corresponds to linearly bonded CO and state (II) to multibonded.

atoms (16). Bridged nitrosyl complexes are less common than bridged carbonyl compounds. Such complexes are responsible for a ν NO band close to 1500 cm^{-1}.

(iii) Adsorption in a bent form with NO bonded by the nitrogen atom end. Such species are associated with a NO^- structure and lead to a ν NO band located between 1500 and 1700 cm^{-1}.

In the case of the Pd/SiO_2 catalyst (Fig. 7a), the IR spectrum of adsorbed NO is similar to that reported by Moriki *et al.* (17). It shows three bands at 1740 cm^{-1} (strong), 1660 cm^{-1} (strong), and 1570 cm^{-1} (weak). The 1740 cm^{-1} band is assigned to NO linearly adsorbed on one surface palladium atom, whereas the 1660 cm^{-1} band can be tentatively attributed to NO bonded to one palladium atom in the bent form. In the spectra of NO adsorbed on silica-supported Pd–Ag and Pd–Cr alloys (Figs. 7b and 7c), the bands at 1740 and 1660 cm^{-1} are still observed. In contrast, the 1570 cm^{-1} band has disappeared. Such behavior might be explained by a dilution effect of palla-

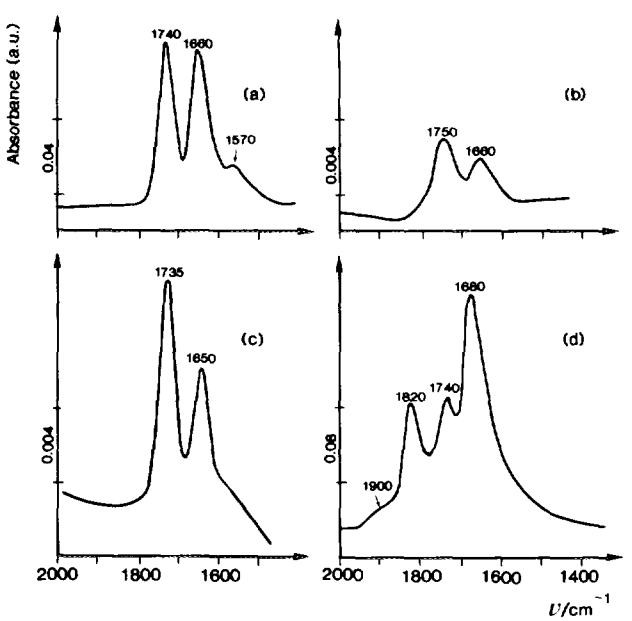

FIG. 7. IR spectra of NO adsorbed at 300 K: (a) on Pd, (b) on Pd–Ag, (c) on Pd–Cr, and (d) on Rh.

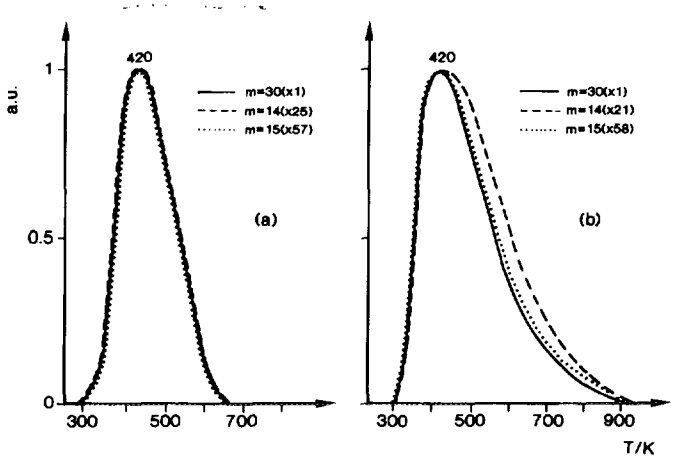

FIG. 8. Thermodesorption of NO adsorbed at 300 K: (a) on Pd, and (b) on Rh.

dium atom ensembles by silver or chromium atoms. In such a case, the 1570 cm^{-1} band observed on the Pd/SiO_2 sample could be assigned to NO bridge-bonded between two palladium atoms.

The IR spectrum of NO adsorbed at room temperature on the Rh/Al_2O_3 sample (Fig. 7d) shows four bands: 1900 cm^{-1} (very weak), 1820 and 1740 cm^{-1} (medium), and 1680 cm^{-1} (strong). The doublet at 1820 and 1740 cm^{-1} was previously attributed to a surface rhodium dinitrosyl complex (18, 19). The conditions of formation of the 1900 cm^{-1} band were carefully described by Anderson *et al.* (20). The intensity of that band strongly increased after treatment of a Rh/Al_2O_3 sample under CO at 200°C or by room temperature adsorption of NO on a rhodium surface previously covered by oxygen. The 1900 cm^{-1} band has been assigned to NO adsorbed onto rhodium in an ionic state. In our experiments, the very weak intensity of that band showed that the dissociation of NO onto metallic rhodium is quite limited. Finally, the 1680 cm^{-1} band could be due to a side-reaction with the alumina support leading to the formation of nitrato or nitrito groups. However, such species show additional bands in the 1700–1200 cm^{-1} range which are not observed. Thus, the 1680 cm^{-1} band could be tentatively attributed to NO bonded to rhodium atoms in a bent form as already proposed in Ref. (21).

TABLE 3

Thermodesorption of NO Adsorbed at 300 K

Sample	T (K)	$\%N_2$
Pd/SiO_2	420	≈0
$Pd–Ag/SiO_2$	390	≈0
$Pd–Cr/SiO_2$	410	≈5
Rh/Al_2O_3	420	≈10

The thermodesorption curves of NO adsorbed at 300 K on Pd and Rh are represented in Figs. 8a and 8b. Following the diagram of the fission products mentioned above, the recording of the 30, 15, and 14 masses leads to the proportion of NO evolved without decomposition. Indeed, for Pd, the three curves can be superimposed, which is not the case for Rh. One can conclude that NO is not decomposed on Pd and that 20% is converted into N_2 on Rh. This relatively low degree of NO dissociation on Rh compared to the results of other authors (22) reporting a value of 50% is surprising. However, in our case the experiments are performed in the absence of stainless steel (in a quartz vessel) and the high pumping speed avoids the readsorption of NO. This can explain the difference.

On Pd–Ag, as on Pd, NO is not decomposed. However, Pd–Cr has the same behaviour as Rh and converts 15% of the NO to N_2. These results are summarized in Table 3.

(V) CO–NO Coadsorption at 300 K and Thermoreaction at 430 K

The results of the thermodesorption experiments performed after adsorption at 300 K of an equimolecular CO–NO mixture are gathered in Table 4. The first observation is that the amount of evolved NO is in all cases much larger than that of CO, especially on Pd-based catalysts. Compared to pure palladium, the effect of Ag is to increase this NO/CO ratio still further and that of Cr to slightly decrease it. The adsorption strength of NO as

TABLE 4

Thermodesorption of CO and NO Adsorbed at 300 K

	NO Desorption (K)		CO Desorption (K)			
Sample	Alone	CO/NO = 1	Alone	CO/NO = 1	NO/CO	$\%N_2$
Pd/SiO_2	420	440	390, 590	390, 570	≈13	≈0
$Pd–Ag/SiO_2$	390	390	410, 620	360, 620	≈22	≈0
$Pd–Cr/SiO_2$	410	400	420, 550	370, 490	≈11	≈4
Rh/Al_2O_3	420	410	420, 550	370, 500	≈4	≈13

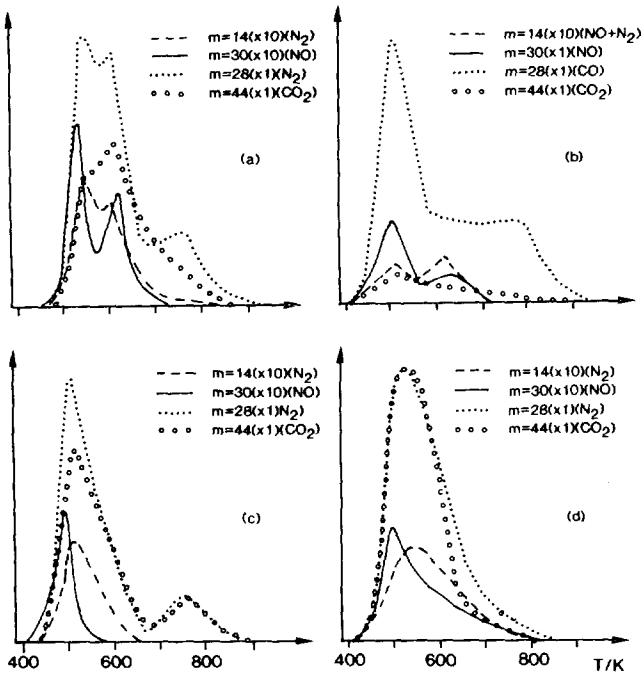

FIG. 9. Thermodesorption after adsorption of an equimolecular mixture of CO–NO mixture at 430 K: (a) on Pd, (b) on Pd–Ag, (c) on Pd–Cr, and (d) on Rh.

deduced from the temperature maximum of the desorption peak is only slightly modified by the presence of CO. In contrast, a shift to low temperature of the desorption peak of CO occurs in the presence of NO on Pd–Cr and Rh. The fraction of NO converted to N_2 during the desorption is not significantly changed compared to the measurement in the absence of CO.

Obviously an adsorption temperature of 300 K is too low to give rise to a significant amount of NO dissociation. After several tests it was found that, if the chemisorption of the reaction mixture is performed at 430 K on the reference Rh catalyst, only CO_2 and N_2 are evolved. An equimolecular mixture of CO and NO was thus admitted at 430 K on all the catalysts. The corresponding thermodesorption curves are shown in Fig. 9 for the 44, 30, 28, and 14 masses. The separation between N_2 and NO is achieved after the calibration mentioned above. It can be concluded from inspection of the different curves that mainly CO_2 and N_2 are evolved on Pd, Pd–Cr, and Rh, and mainly CO and NO on Pd–Ag. On Pd–Cr and Rh, N_2 and CO_2 are evolved simultaneously around 530 K, whereas on pure palladium two desorption peaks of simultaneous release of these two molecules are observed at 560 and 620 K. On Pd–Ag, the amount of evolved CO_2 is 6–8 times lower than on Pd–Cr and the desorption peak of NO is located at the same temperature as in the absence of CO, which confirms the weak interaction between the two molecules. Finally, no significant amounts of N_2O are ever detected during these desorption experiments.

DISCUSSION

To understand the effect of the surface composition on the CO–NO interaction, the following steps leading to the formation of CO_2 and N_2 should be considered (22, 23):

$$NO \rightleftharpoons NO_{ads} \quad [1]$$

$$NO_{ads} \rightleftharpoons N_{ads} + O_{ads} \quad [2]$$

$$CO \rightleftharpoons CO_{ads} \quad [3]$$

$$NO_{ads} + N_{ads} \rightarrow N_2(gas) + O_{ads} \quad [4]$$

$$2N_{ads} \rightarrow N_2(gas) \quad [5]$$

$$CO_{ads} + O_{ads} \rightarrow CO_2. \quad [6]$$

Obviously, as shown above, the dissociative adsorption of NO following reaction [2] is negligible at 300 K even on Rh, where less than about 9% of NO is adsorbed dissociatively (23). On the Pd-based catalysts, the molecular adsorption following reaction [1] leads to the desorption of molecular NO at low temperature, 420 K. When the adsorption is performed at 430 K, the dissociative adsorption occurs partially but the temperature increase during the thermodesorption displaces reaction [2] to the left and NO is desorbed, but at higher temperature, 500 K.

The low amount of CO_2 and N_2 collected on Pd–Ag indicates that the rates of reactions [4]–[6] are extremely low, probably because the surface coverage by N_{ads} and O_{ads} produced by reaction [2] is low. Also as shown above, the coverage by CO in the presence of NO is low.

On the other catalysts, the formation of N_2 and CO_2 occurs, probably via reaction [4] and [6], which have a measurable rate at relatively low temperature. This is not the case for reaction [5], known to occur at higher temperature (22, 24, 25).

Now if one considers the global reaction

$$CO + NO \rightarrow CO_2 + \tfrac{1}{2}N_2, \quad [7]$$

the CO_2/N_2 ratio should be equal to 2, which is not the case, since ratios of 0.6, 0.7, and 1.3 are respectively measured on the Pd, Pd–Cr, and Rh catalysts. Actually, since N_2 is formed preferentially by reaction [4] and CO_2 by reaction [6], N_2 formation is related to the fraction of NO dissociatively adsorbed, while the formation of CO_2 would depend on the *amount* of CO *available* on the surface. Therefore, one can conclude that the deficit of CO_2 can be ascribed to an amount of chemisorbed CO too low to consume all the oxygen produced by reaction [4].

However, thermodesorption has shown that the binding energies of linearly adsorbed CO and of NO are similar

on all the catalysts, with desorption temperatures around 400 K. Multibonded (MB) CO is evolved at higher temperature, between 550 and 620 K. These two forms are present in similar proportion on pure Pd and Rh. Infrared spectroscopy confirms that the presence of Cr and especially that of Ag reduces the proportion of MB CO. Surprisingly, the IR study of the sequential adsorption of these two reactants shows that they are to a large extent displaced by each other; only on Rh and Pd–Cr does a small fraction of the MB form of CO remain on the surface after the introduction of NO. One must assume that NO strongly modifies the adsorption of CO, probably by decreasing the number of free polyatomic adsorption sites or, as has been shown in the case of rhodium, by upsetting totally the structure of the particles (26). However, this effect of NO is also observed on the desorption of linear CO, which occurs 30 to 50 K lower than on the clean surface. This decrease of 20 to 30% of the adsorption energy might be due either to repulsive interactions between CO and N_{ads}, or to adsorption on partially oxidized surface. The final result is that the CO/NO ratio on the surface measured after coadsorption at 300 K of an equimolecular mixture of the two gases is low, varying from 0.25 on Rh, to 0.09 on Pd–Cr, 0.08 on Pd, and 0.05 on Pd–Ag.

The situation concerning the relative coverage is different when the thermoreaction is performed at 430 K. On Pd–Ag, where the conversion does not take place, three times more CO than NO is evolved. In contrast, on the other catalysts which mainly lead to CO_2 and N_2, the ratio of CO_2 to N_2, although increasing from Pd, Pd–Cr, and Rh, remains lower than 2, as should be mandated by the stoichiometry of reaction [7]. This means that the fraction of the surface covered by CO is in all cases lower than that covered by NO. Since the amount of NO collected during the desorption is not larger than 5 to 7%, it should be converted to N_2 via reaction [4], leaving on the surface the excess of chemisorbed oxygen not consumed by reaction [6].

An intriguing feature of the thermograms measured after coadsorption at 430 K is the fact that both desorption of CO_2 and N_2 occur at the same temperature on Pd–Cr and Rh, 530 K, which is not the case on pure Pd. Two possible explanations can be put forward: either the surface diffusion of adsorbed CO or O is faster than on the other catalysts or, more likely, the dissociation of NO occurs at lower temperature on these two solids.

Effect of the Second Metal

This discussion on the reaction mechanism based on thermoreaction experiments has shown that to obtain a good yield for reaction [7], two conditions have to be fulfilled.

First, the two adsorbates, CO and NO, have to be present simultaneously on the surface. This is indeed the case on rhodium and less on palladium on which only 10% of CO is chemisorbed in the presence of NO at 300 K. The situation is still worse when silver is alloyed to palladium. This effect can be ascribed to the large silver surface concentration after equilibration above 600 K, which is shown by the X-ray study. In contrast, the presence of chromium slightly improves the CO coverage.

Second, the metal surface should dissociate NO so that reactions [4] and [6] can proceed. Once again the effect of silver is unfavourable, since on Pd–Ag only CO and NO are evolved. This is due to the large silver migration at the surface of the catalyst. In contrast, chromium certainly promotes the NO dissociation; compared to pure palladium, a larger fraction of NO is converted (96% compared to 90%), but more interestingly, CO_2 and N_2 are evolved simultaneously and at a lower temperature than on the pure metal. Only a strong effect of this element on the electronic properties of palladium can account for such modifications of the chemisorptive properties by the addition of only 13 at.% of chromium to palladium.

CONCLUSIONS

Infrared and thermoreaction experiments have clearly shown that the CO–NO conversion is first governed by the competitive adsorption of the two reactants; in spite of adsorption energies, which are similar, the surface coverage by CO is low in the presence of NO on palladium, compared to rhodium. This coverage is decreased still further by alloying palladium with silver. In contrast, the presence of chromium slightly increases the CO/NO surface ratio. The thermoreaction experiments have clearly shown that the dissociative adsorption of NO and the reaction between CO and O adsorbed species are the important steps of the mechanism. The analysis of the evolved products has shown that dissociation does not occur on Pd–Ag and that it is improved on Pd–Cr, compared to pure Pd. Under these static conditions, the Pd–Cr alloy has a behaviour close to that of Rh.

In a future publication, the reactivity of these solids under a flow of reactants containing variable proportions of oxygen will be described in order to approach more realistic conditions (27).

REFERENCES

1. Taylor, K. C., Automotive Catalytic Converters; *in* "Catalysis: Science and Technology," (J. R. Anderson and M. Boudart, Eds.), Vol. 5. Springer-Verlag, Berlin, 1984. *Catal. Rev. Sci. Eng.* **35,** 457 (1993).
2. Schlatter, J. C., and Taylor, K. C., *J. Catal.* **49,** 42 (1977).

3. Oh, S. H., and Carpentier, J. E., *J. Catal.* **98,** 178 (1986).
4. McCabe, R. W., and Mitchell, P. J., *Appl. Catal.* **27,** 83 (1986).
5. Borgna, A., Moraweck, B., Massardier, J., and Renouprez, A. J., *J. Catal.* **128,** 99 (1991).
6. Massardier, J., Bertolini, J. C., and Renouprez, A. J., *in* "Proceedings, 9th International Congress on Catalysis, Calgary, 1988," (M. J. Phillips and M. Ternan, Eds.), Vol. 3, p. 1222. Chem. Inst. Canada, Ottawa, 1988.
7. Soma-Moto, Y., and Sachtler, W. M. H., *J. Catal.* **32,** 315 (1974); Primet, M., Mathieu, M. V., and Sachtler, W. M. H., *J. Catal.* **44,** 324 (1976).
8. Bradshaw, A. M., and Hoffmann, F. M., *Surf. Sci.* **72,** 513 (1978).
9. Yang, C., and Garland, C. W., *J. Phys. Chem.* **61,** 1504 (1957).
10. Coles, B. R., *J. Inst. Mater.* **84,** 346 (1956).
11. Miedema, A. R., *Z. Metalklkd.* **69,** 455 (1978).
12. Wicke, E., and Brodowski, H., *in* "Topics in Applied Physics," Springer-Verlag, Berlin, **29,** 73 (1978).
13. Primet, M., *J. Chem. Soc., Faraday Trans. 1* **74,** 2570 (1978).
14. Cotton, F. A., and Wilkinson, G., Advanced Inorganic Chemistry, 3rd Edition, p. 713. Interscience, New York, 1972.
15. Finn, P., and Jolly, W. L., *Inorg. Chem.* **11,** 893 (1972).
16. Norton, J. R., Colmann, J. P., Dolcett, G., and Robinson, T., *Inorg. Chem.* **11,** 382 (1972).
17. Moriki, S., Inoue, Y., Miraki, E., and Yasumori, J., *J. Chem. Soc., Faraday Trans. 1* **78,** 171 (1982).
18. Hyde, E. A., Rudham, R., and Rochester, C. H., *J. Chem. Soc., Faraday Trans. 1* **80,** 531 (1984).
19. Liang, J., Wang, H. P., and Spicer, L. D., *J. Phys. Chem.* **89,** 5840 (1985).
20. Anderson, J. A., Millar, G. J., and Rochester, C. H., *J. Chem. Soc., Faraday Trans. 1* **86,** 571 (1990).
21. Arai, H., and Tominaga, H., *J. Catal.* **43,** 131 (1976).
22. Oh, S. H., Fisher, G. B., Carpenter, J. E., and Goodman, D. W., *J. Catal.* **100,** 360 (1986).
23. Chin, A. A., and Bell, A. T., *J. Phys. Chem.* **87,** 3700 (1983).
24. Root, T. W., Schmidt, L. D., and Fisher, G. B., *Surf. Sci.* **134,** 30 (1983).
25. Campbell, C. T., and White, J. M., *Appl. Surf. Sci.* **1,** 347 (1978).
26. Solymosi, F., Bangasi, T., and Novak, E., *J. Catal.* **112,** 183 (1988).
27. El Hamdaoui, A., *et al.* to be submitted.